Alkali polyphosphates as new potential materials for thermal energy storage

Doan Pham Minh, Abdoul Razac Sane, Nawal Semlal, Patrick Sharrock, Ange Nzihou

Alkali polyphosphates as new potential materials for thermal energy storage

Doan Pham Minh[a,*], Abdoul Razac Sane[a], Nawal Semlal[b], Patrick Sharrock[a], Ange Nzihou[a]

[a] Université de Toulouse, Mines Albi, CNRS, Centre RAPSODEE, Campus Jarlard, F-81013 Albi Cedex 09, France
[b] Direction R & D, OCP SA, BP 118, 24000 El Jadida, Morocco

A B S T R A C T

Until now, molten salts (nitrate-based salts) are the main materials for sensible heat storage at industrial scale. The working temperature range of these materials is limited below 500 °C. There is not yet a solution for sensible heat storage at high temperature. This paper aimed to investigate alkali polyphosphates ($(MPO_3)_n$, with M = Li, Na or K) as new promising materials for sensible heat storage at high temperature. Alkali polyphosphates could be formed by dehydration of monoalkali dihydrogenphosphates (MH_2PO_4, with M = Li, Na or K), which occurs below 400 °C. Alkali polyphosphates resulted from this dehydration melted at 628, 657 and 812 °C for sodium, lithium and potassium polyphosphate, respectively. All these liquids evaporated above 900 °C but no destruction of their chemical structure was recorded. Sodium polyphosphate seemed to be the most promising material for sensible heat storage at high temperature because of its large potential working temperature (628–900 °C), its availability and its low cost compared to lithium and potassium polyphosphates. The results open new prospects for the development of the thermal energy storage field.

Keywords:
Alkali polyphosphate
Sensible heat storage
Thermal energy storage

1. Introduction

Energy consumption constantly increases worldwide. This is observed for all types of primary energy including coal, oil, natural gas, nuclear energy, hydroelectricity, and renewable energy. Fossil fuel (coal, oil and natural gas) still remains the world's dominant energy. However, the reserve of fossil fuel is limited with irregular distribution over the world. In addition, the consumption of fossil fuel leads to the emission of carbon dioxide in the atmosphere. Carbon dioxide is the main greenhouse gas (GHG) to cause global warming. Global warming causes serious problems to ecosystems, animal and humans: melting of glaciers leading to the rise in sea level, irregular weather patterns, massive crop failure, animal extinction, frequent wildfires… (Anderson et al., 2016; Arora et al., 2016; Punzón et al., 2016). So, the development of renewable energy is highly recommended for the 21st century and is part of the global strategy for limiting the emission of GHG. The most common renewable energies include solar, biomass, wind, geothermal power or hydropower. Among them, solar energy has the highest potential with the development of photovoltaic (PV) and concentrated solar power (CSP) systems. Nevertheless, solar energy presents also various limits which relate to the intermittence of sunlight, the seasonal character, the irregular distribution between different countries and the dephasing between energy production and consumption. For CSP systems, the development of efficient thermal energy storage (TES) technology is a decisive factor to overcome the limits mentioned above.

TES is generally classified into 3 categories: sensible heat storage, latent heat storage, and thermochemical energy storage (Veerakumar and Sreekumar, 2016; Weinstein et al., 2015). Sensible heat storage consists in the heating of storage media without chemical reaction or phase change. Latent heat includes a phase change which allows a higher energy storage density compared to sensible heat storage. Thermochemical energy storage is based on a reversible reaction with endothermal and exothermal phases. Up-to-date, only sensible heat storage is developed at large industrial scale, and has a high growth rate recently. According to the International Energy Agency (IEA) (2014a), the cumulative CSP capacity worldwide reached around 0.5, 1.6 and 3.9 GW in 2009, 2012 and 2014, respectively. IEA studies also predicted, in their BLUE Map scenario, that in 2050, CSP plants would provide 5% of the annual global electricity production (compared to 6% by solar PV), which shows the potential and interest in solar energy (IEA, 2010, 2014b).

Different materials can be used as media for sensible heat storage. They can be either liquid or solid during the charging and discharging phases. Liquid materials include mineral oil, synthetic oil, silicone oil, liquid sodium, carbonate salts, nitrate and nitrite salts (Gil et al., 2010). The most common commercial liquid material is known as Solar Salt containing 60 wt% $NaNO_3$ and 40 wt% KNO_3 (Fernández and Grageda, 2015; Peiró et al., 2016). It is currently used in different CSP plants such as ANDASOL (Dintera and Gonzalez, 2014; Solar Millenium AG, 2008;

* Corresponding author.
E-mail address: doan.phamminh@mines-albi.fr (D. Pham Minh).

Table 1
List of chemicals used in this work.

Name	Chemical formula	Supplier
Sodium trimetaphosphate	$Na_3P_3O_9$	Aldrich
Sodium dihydrogenphosphate dihydrate	$NaH_2PO_4{\cdot}2H_2O$	Aldrich
Lithium dihydrogenphosphate	LiH_2PO_4	Aldrich
Potassium dihydrogenphosphate	KH_2PO_4	Aldrich

Trabelsi et al., 2016), or GEMASOLAR (Rellosoa and García, 2015). Nitrate salts including Solar Salt have several advantages: (i) they are in liquid state at atmospheric pressure (and high temperature), which facilitates their use in CSP plants as TES material or heat transfer fluid (HTF); (ii) they have a working temperature range (282–386 °C for ANDASOL plants (Dintera and Gonzalez, 2014; Trabelsi et al., 2016) which allows generating vapor for steam turbine; (iii) they are less toxic than organic oils (Fernández and Grageda, 2015). In addition, they have low viscosity and low vapor pressure. However, nitrate salts have also various disadvantages and drawbacks. Their operational temperature is limited at 500 °C to avoid thermal decomposition of nitrate salts (Bauer et al., 2012). They are also used as fertilizer so its massive utilization in CSP plants can affect and compete with agricultural activities. When they are used as TES material, nitrate salts of high quality are recommended to avoid corrosion of tank and other equipment, which usually increases cost of CSP plant (Kuravi et al., 2013). Thus, numerous works have recently been devoted to the improvement of Solar Salt or the development of new materials for sensible heat energy storage (Fernandez et al., 2010; Fernández and Grageda, 2015; Gil et al., 2010; John et al., 2013; Kuravi et al., 2013; Martins et al., 2015).

This work focused on the development of several alkali polyphosphates $((MPO_3)_n)$, with M = Na, K, or Li) as liquid media for sensible heat storage. In the literature, much work was reported on the investigation of nitrate salts, halogenated salts, carbonate salts, sulfates salts, metals and metal oxides (Hoshi et al., 2005). However, to the best our knowledge, there is no work reported yet on liquid (poly)phosphate-based products as TES materials. (Poly)phosphate-based products constitute a large family of inorganic salts with interesting physico-chemical and thermal properties, in particularly their low corrosion and high thermal stability compared to other inorganic salts.

2. Materials and methods

Table 1 summaries the chemicals used in this work. They were all provided by Aldrich, with high purity for R & D purpose. All these chemicals were in fine powder form. They were used as received without further modification.

TG-DTA analysis was performed with a TA Instruments SDTQ600 analyzer with the heating rate of 5 °C min^{-1} under air flux (100 mL min^{-1}). Platinum crucibles of 3 mm of diameter and 3 mm of height were used. For each analysis, around exactly 10–15 mg of solid was needed. In general, the instrument used can measure masse change and heat flow of the analysis (W/g). However, it was only used as TG-DTA analyzer in this work. In fact, heating alkali phosphates (MH_2PO_4 with M = Li, Na, or K) leads to the formation of alkali polyphosphates ($(MPO_3)_n$) as shown thereafter in the Results section. When alkali polyphosphate melts, it exists in liquid state which can affect the weight signal. In addition, liquid polyphosphate could overflow the platinum crucible and then stick it on the microbalance of the TG-DTA apparatus. In this case, the microbalance has to be changed. To solve this problem, fine alumina powder was set on the surface of the microbalance to avoid the direct contact of the platinum crucible with the microbalance. Thus, the platinum crucible could be easily removed after TG-DTA test, despite eventual overflow of alkali polyphosphates. But the presence of alumina power disturbs the heat change signal. Thus, only DTA curves could be obtained, instead of DSC curves.

FTIR spectra were recorded with a Shimadzu FTIR 8400 S spectrometer, using a sensitive pyroelectric detector with a l–alanine–doped deuterated triglycine sulfate (DLATGS) element (maximum resolution of 0.85 cm^{-1}, signal-to-noise ratio of 20,000: 1). The measurement was carried out directly with solid sample under powder form. Solid recovered from TG-DTA analysis was quickly analyzed by FTIR without further preparation.

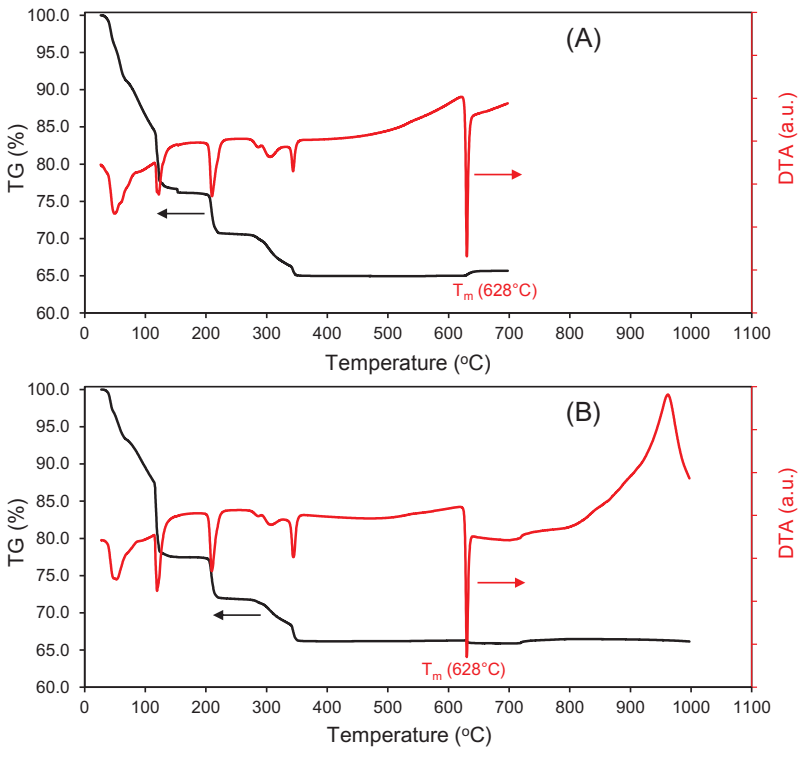

Fig. 1. TG-DTA under air atmosphere with the heating rate of 5 °C min^{-1} of $NaH_2PO_4{\cdot}2H_2O$ up to 700 °C (A) and 1000 °C (B).

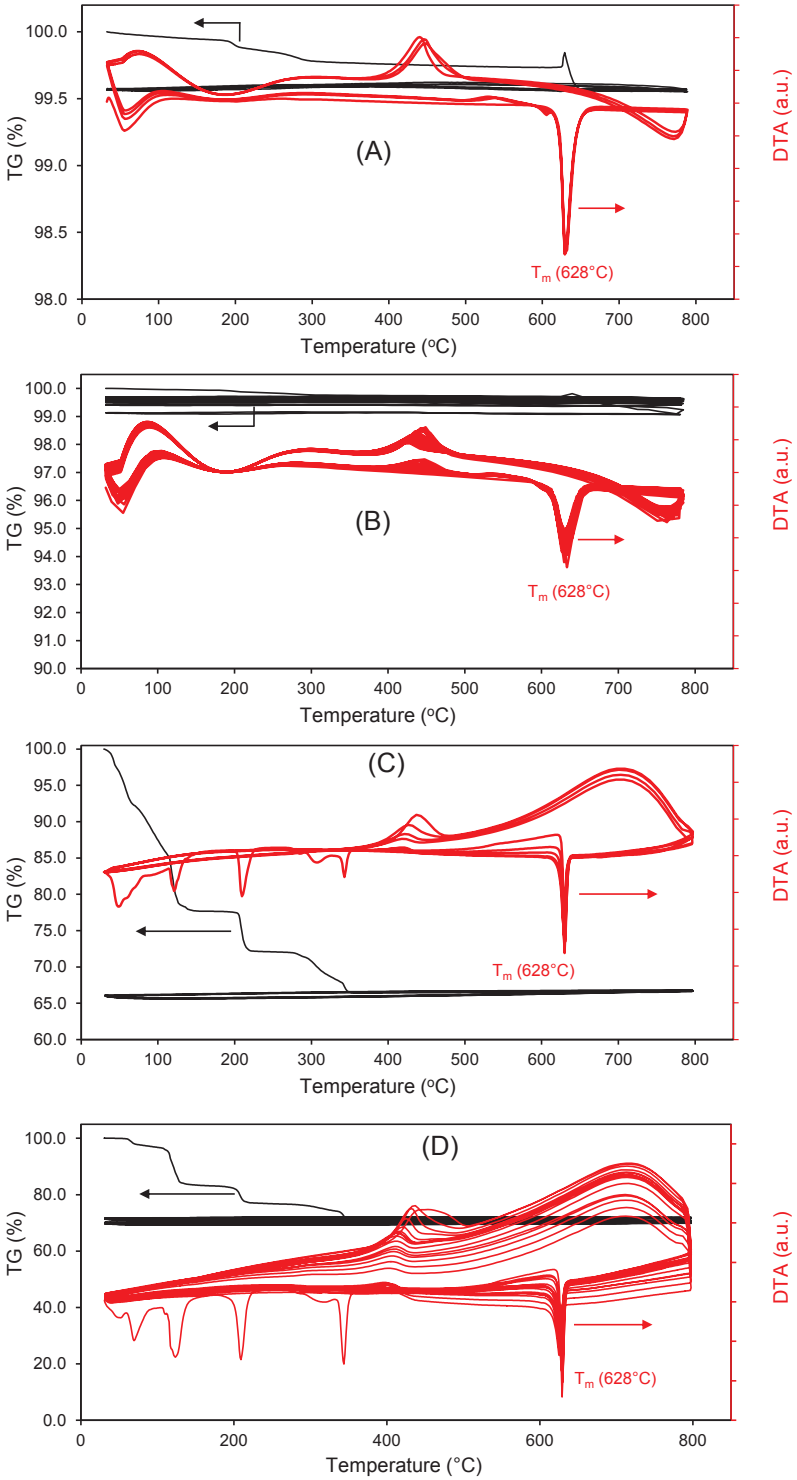

Fig. 2. TG-DTA cycle analysis under air atmosphere with the heating rate of 5 °C min^{-1} of: (A and B) $Na_3P_3O_9$; (C and D) $NaH_2PO_4{\cdot}2H_2O$.

3. Results

3.1. Characterization of sodium polyphosphate, $(NaPO_3)_n$

Fig. 1 shows TG-DTA curved of $NaH_2PO_4{\cdot}2H_2O$ under air flux in the temperature range of 30–700 °C (A) or 30–1000 °C (B).

This compound decomposed by dehydrations as follows:

$$NaH_2PO_4{\cdot}2H_2O \rightarrow NaH_2PO_4{\cdot}H_2O + H_2O \quad (1)$$

$$NaH_2PO_4{\cdot}H_2O \rightarrow NaH_2PO_4 + H_2O \quad (2)$$

$$NaH_2PO_4 \rightarrow NaPO_3{\cdot}1/2H_2O + 1/2H_2O \quad (3)$$

$$NaPO_3{\cdot}1/2H_2O \rightarrow NaPO_3 + 1/2H_2O \quad (4)$$

The first two weight losses took place at the temperature range of 30–145 °C, and corresponded to the dehydration of crystalized water. The last two weight losses were due to the condensation of dihydrogenophosphate anions ($H_2PO_4^-$), which happened in the temperature range of 190–350 °C. For each weight loss, the value recorded by TG-DTA apparatus was close to the theoretical value calculated for this compound (11.5 wt% for the first two weight losses, and 5.8 wt% for the last two weight losses). Sodium polyphosphate, $(NaPO_3)_n$, was

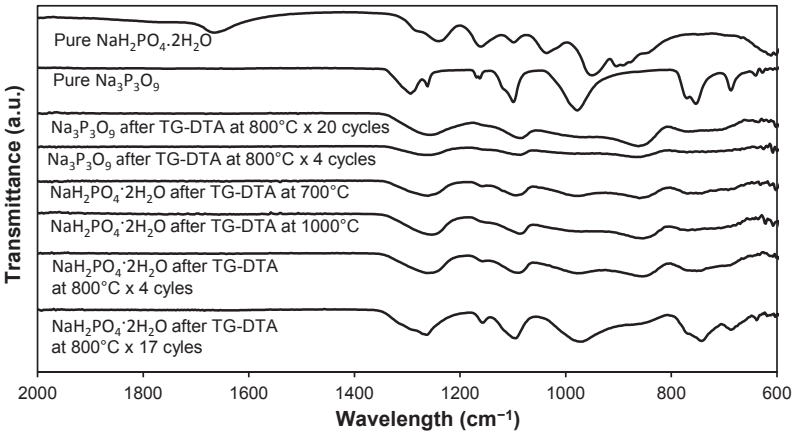

Fig. 3. FTIR spectra of $Na_3P_3O_9$ and $NaH_2PO_4{\cdot}2H_2O$ before and after TG-DTA analysis.

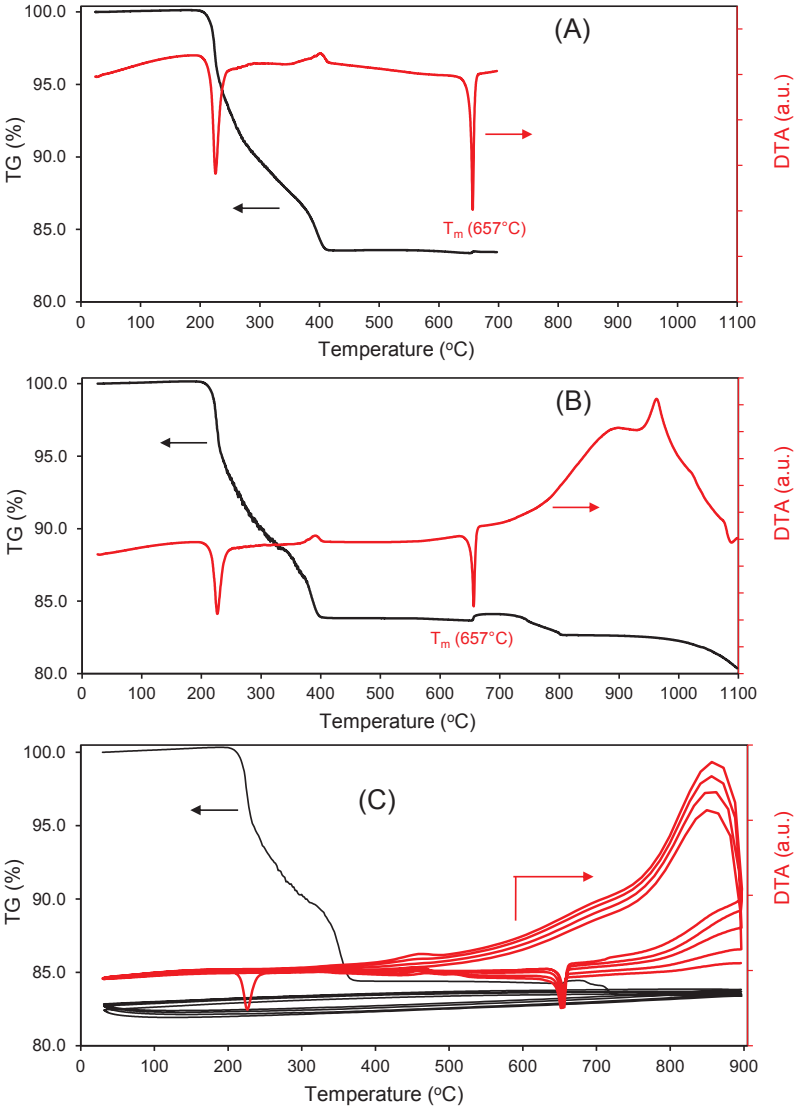

Fig. 4. TG-DTA of LiH_2PO_4 under air atmosphere with the heating rate of 5 °C min^{-1}.

expected as the product of the condensation. This product was thermally stable below 628 °C without notable weight loss. Then, it melted to give the DTA peak at 628 °C. This phenomenon slightly disturbed the signal of the microbalance of TG measurement. Finally, sodium polyphosphate seemed to evaporate above 900 °C (Fig. 1(B)). In the temperature of 628–900 °C, no weight loss was observed. TG-DTA was repeated several times to confirm the repeatability of the analysis. The similarity of TG and DTA curves of Fig. 1(A) and (B) illustrates this repeatability.

Fig. 2 shows TG-DTA curves of $Na_3P_3O_9$ and $NaH_2PO_4{\cdot}2H_2O$ with 4, 17 or 20 consecutive heating-cooling cycles in the temperature range of 30–800 °C. For $Na_3P_3O_9$ (Fig. 2(A) and (B)), the first heating step led to some small weight losses (< 0.5 wt%) and the melting at 628 °C. For the next cooling and heating steps, there was no notable weight loss

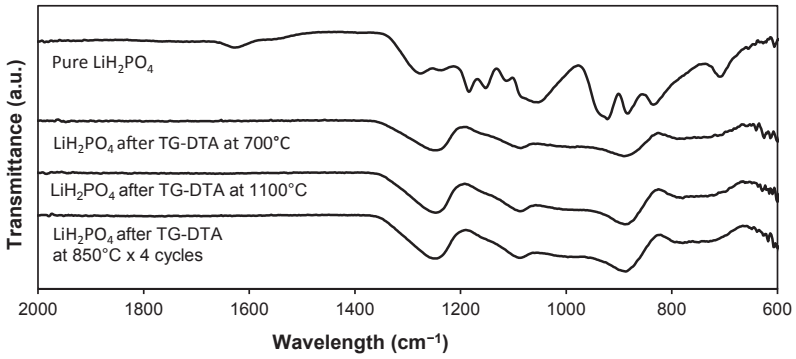

Fig. 5. FTIR spectra of synthesized $LiPO_3$ before and after TG-DTA analysis.

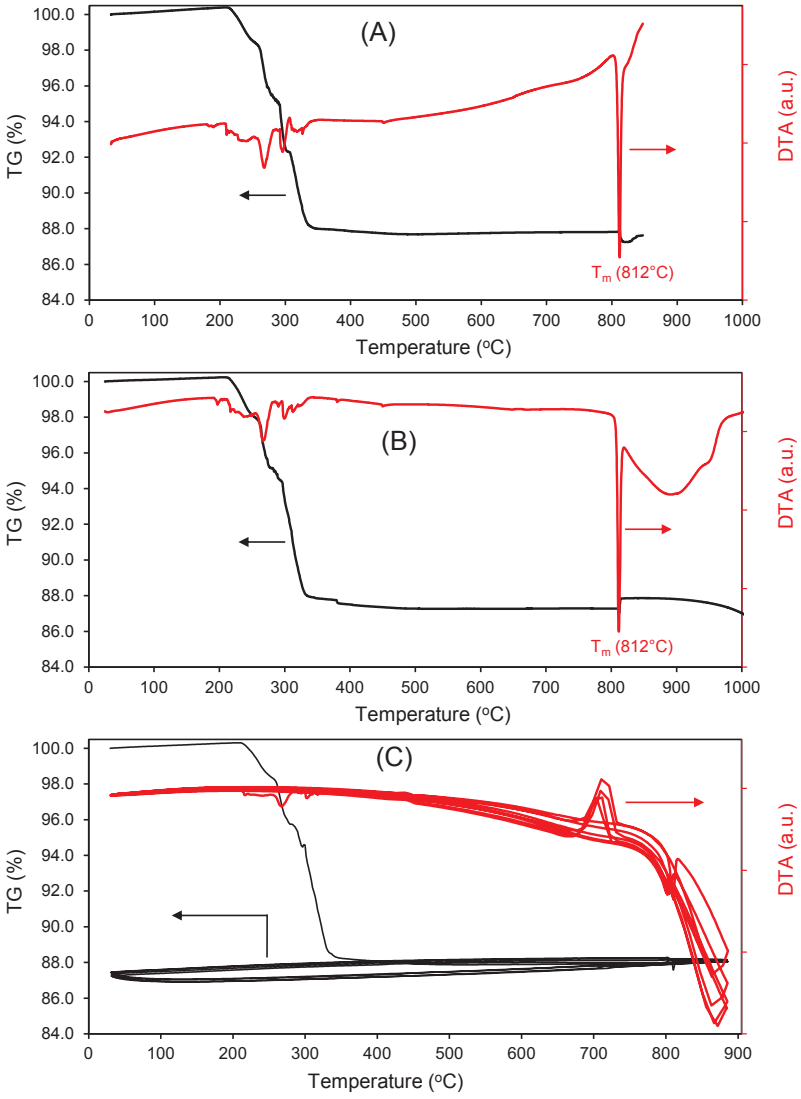

Fig. 6. TG-DTA of KH_2PO_4 under air atmosphere with the heating rate of 5 °C min^{-1}.

which demonstrated the thermal stability of the resulting product, $(NaPO_3)_n$, within the temperature range studied. The results were repeated for both the analyses with 4 and 20 consecutive heating-cooling cycles. Further FTIR analysis shows that no significant change was observed inside its structure (Fig. 3). For $NaH_2PO_4{\cdot}2H_2O$ (Fig. 2 (C) and (D)), the first heating step led to different dehydrations as mentioned previously, as well as the melting at 628 °C. Then, $(NaPO_3)_n$ formed from this step was thermally stable during 4 or 17 heating-cooling cycles.

Fig. 3 shows FTIR spectra of $Na_3P_3O_9$ and $NaH_2PO_4{\cdot}2H_2O$ before and after TG-DTA analyses. As mentioned above, the heating of $Na_3P_3O_9$ and $NaH_2PO_4{\cdot}2H_2O$ above 628 °C led to the melting of these salts and the formation of sodium polyphosphate, $(NaPO_3)_n$. The structure of $(NaPO_3)_n$ seemed to be similar after being heated to different temperatures of 700, 800 or 1000 °C. In fact, FTIR analysis shows that all the solids recovered from TG-DTA analysis had similar spectra. FTIR analysis illustrated also the structural change of $Na_3P_3O_9$ to more stable form ($(NaPO_3)_n$) after melting at 628 °C, due to the oligomerization or polymerization of $NaPO_3$ unit.

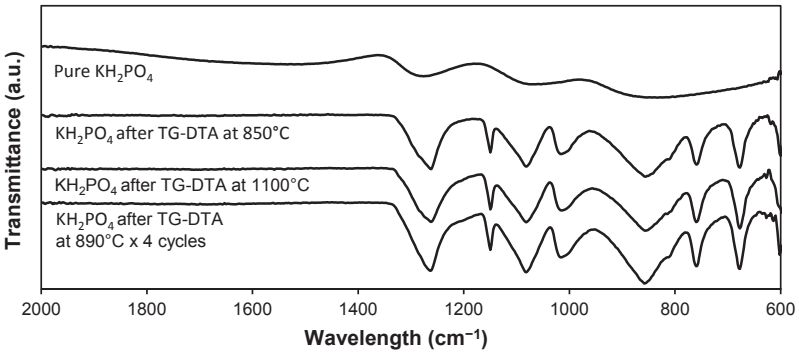

Fig. 7. FTIR spectra of synthesized KPO_3 before and after TG-DTA analysis.

3.2. Characterization of lithium polyphosphate, $(LiPO_3)_n$

Fig. 4 shows TG-DTA analysis of LiH_2PO_4 under air atmosphere. LiH_2PO_4 had a progressive dehydration in the temperature range of 200–415 °C (at the heating rate of 5 °C min^{-1}). The maximum of DTA signal of this dehydration was found at 225.5 °C. The weight loss of this dehydration was recorded around 17 wt%, which corresponds to the following equation:

$$LiH_2PO_4 \rightarrow LiPO_3 + H_2O \quad (5)$$

$LiPO_3$ resulting from this dehydration melted at 657 °C. As previously observed with $NaPO_3$, this melting caused a perturbation of TG signal. At liquid state, $LiPO_3$ was thermally stable up to around 900 °C before its evaporation, as observed in Fig. 4(B). Thus, consecutive heating-cooling cycles was then performed with LiH_2PO_4 in the temperature range of 30–900 °C (Fig. 4(C)). Any notable weight loss was observed after the first heating step. Also, the maximum of DTA peak was constant at 657 °C indicating that there was probably no structural change of $LiPO_3$ after its formation by the first melting at 657 °C.

Fig. 5 shows FTIR spectra of the initial LiH_2PO_4 powder and the solids recovered from TG-DTA analysis. LiH_2PO_4 had several peaks at 1300–700 cm^{-1}, which must be due to P – O vibrations. For the solids recovered from TG-DTA analyses, all the spectra were similar to each other, and did not depend on the final temperature of TG-DTA analysis. In particular, as observed previously, TG-DTA analysis at 30–1100 °C showed the partial evaporation of $(LiPO_3)_n$ above 900 °C. We suppose that this evaporation did not cause any notable change in the structure of the remaining solid because its FTIR spectrum was also similar to those of the solids treated at lower temperatures.

3.3. Characterization of potassium polyphosphate, $(KPO_3)_n$

TG-DTA analysis of KH_2PO_4 is presented in Fig. 6. The dehydration of this compound took place in the temperature range of 210–350 °C. This dehydration seemed to happen in several consecutive steps as indicated by the presence of multiple DTA peaks. The global weight loss at 210–350 °C reached approximatively 13 wt% and corresponded to the following equation:

$$KH_2PO_4 \rightarrow KPO_3 + H_2O \quad (6)$$

Thus, KPO_3 was formed above 350 °C. This compound did not show any notable change up to 812 °C, where it melted. The disturbance of the melting step on TG signal was again observed. Liquid KPO_3 was thermally stable up to around 900 °C. Then, it evaporated above 900 °C as observed in Fig. 6 (B).

Fig. 6 (C) shows heating-cooling cycles of KH_2PO_4. The dehydration of KH_2PO_4 was again confirmed during the first heating step. When KPO_3 was formed, it remained thermally stable during repeated heating-cooling cycles.

Fig. 7 presents FTIR spectra of the initial KH_2PO_4 and the solids recovered after TG-DTA analyses. For KH_2PO_4, peaks of P – O vibration were also observed at the wavelength of around 1300–700 cm^{-1}. For the solids recovered from TG-DTA analyses, their FTIR spectra were similar to each other, indicating the structural similarity of these melted solids. In other words, the formation of the same potassium polyphosphate, $(KPO_3)_n$, was expected after its melting point at 812 °C and its structure was stable even above its evaporation temperature.

For a conventional CSP system using molten salt as TES material, the working temperature required is limited between around 281–386 °C, as previously mentioned. These nitrate-based salts are up-to-date the main commercial products for sensible heat storage. There is no available solution for TES at higher temperatures yet. Current research is focused on the development of refractory concretes and ceramics as new TES materials (Fernandez et al., 2010; Fernández and Grageda, 2015; Gil et al., 2010; John et al., 2013; Kuravi et al., 2013; Martins et al., 2015). However, these materials still need improvements mostly concerning their low thermal conductivity, their difficulty for shaping, or their high cost. So, this work demonstrated that liquid alkali polyphosphates could be an interesting solution for sensible heat storage at high temperatures. Among three monoalkali polyphosphates studied, sodium polyphosphate ($(NaPO_3)_n$) seemed to be the most interesting product. It melts at 628 °C and could be stable up to around 900 °C. The melting point of lithium polyphosphate ($(LiPO_3)_n$) is close to that of sodium polyphosphate and this compound is also stable up to around 900 °C. But in general, lithium compounds are less available and more expensive than sodium compounds. As for potassium polyphosphate ($(KPO_3)_n$), it melts at 812 °C and evaporates above 900 °C. So this compound seems to be not convenient for sensible heat storage because of the narrow temperature range wherein it is stable in liquid state.

4. Conclusions

For the first time, alkali polyphosphates were investigated as liquid media for sensible heat storage at high temperature. Alkali polyphosphates ($(MPO_3)_n$, with M = Li, Na or K) could be easily obtained from the dehydration of the corresponding monoalkali dihydrogenphosphate (MH_2PO_4, M = Li, Na, K). After their melting point, alkali polyphosphates were thermally stable up to around 900 °C. Above 900 °C, alkali polyphosphates evaporated, but no chemical decomposition took place. Sodium polyphosphate was the most promising product thanks to its large temperature range in the liquid state (628–900 °C), its availability and its low cost compared to lithium or potassium poly phosphates.

Further work should determine physico-chemical properties for these alkali polyphosphates in liquid state such as heat capacity, thermal conductivity, density, viscosity, corrosive property etc. These data would allow the design of a new solution for sensible heat storage at high temperature.

Acknowledgment

The authors would like to acknowledge the financial support from Prayon and OCP S.A Group, and ANRT (Association Nationale de la

Recherche et de la Technologie, France). The authors gratefully thank colleagues at the RAPSODEE research center, CNRS UMR 5302, for technical help.

References

Anderson, T.R., Hawkins, E., Jones, P.D., 2016. CO_2, the greenhouse effect and global warming: from the pioneering work of Arrhenius and Callendar to today's earth system models. Endeavour 40 (3), 178–187.

Arora, A., Rao, S.A., Chattopadhyay, R., Goswami, T., George, G., Sabeerali, C.T., 2016. Role of Indian Ocean SST variability on the recent global warming hiatus. Glob. Planet. Change 143, 21–30.

Bauer, T., Breidenbach, N., Pfleger, N., Laing, D., 2012. Overview of molten salt storage systems and material development for solar thermal power plants. In: Presented at the 2012 National Solar Conference (SOLAR 2012), Denver CO.

Dintera, F., Gonzalez, D.M., 2014. Operability, reliability and economic benefits of CSP with thermal energy storage: first year of operation of ANDASOL 3. Energy Proc. 49, 2472–2481.

Fernandez, A.I., Martiez, M., Segarra, M., Martorell, I., Cabeza, L.F., 2010. Selection of materials with potential in sensible thermal energy storage. Solar Energy. Mater. Solar Cells 94, 1723–1729.

Fernández, U.A.G., Grageda, M., 2015. 3 – Using molten salts and other liquid sensible storage media in thermal energy storage (TES) systems. In: Advances in Thermal Energy Storage Systems. Woodhead Publishing, pp. 49–63.

Gil, A., Medrano, M., Martorell, I., Lazaro, A., Dolado, P., Zalba, B., Cabeza, L.F., 2010. State of the art on high temperature thermal energy storage for power generation. Part 1 – Concepts, materials and modellization. Renew. Sustain. Energy Rev. 14, 31–55.

Hoshi, A., Mills, D.R., Bittar, A., Saitoh, T.S., 2005. Screening of high melting point phase change materials (PCM) in solar thermal concentrating technology based on CLFR. Solar Energy 79, 332–339.

IAE, 2010. International Energy Agency, Technology roadmap_Concentrating solar power, Paris, France.

IAE, 2014a. < http://www.iea.org/publications/freepublications/publication/technologyroadmapsolarthermalelectricity_2014edition.pdf > (accessed on July 07, 2017).

IAE, 2014b. International Energy Agency, Technology roadmap_Solar photovoltaic energy, Paris, France.

John, E., Hale, M., Selvam, P., 2013. Concrete as a thermal energy storage medium for thermocline solar energy storage systems. Solar Energy 96, 194–204.

Kuravi, S., Trahan, J., Goswami, D.Y., Rahman, M.M., Stefanakos, E.K., 2013. Thermal energy storage technologies and systems for concentrating solar power plants. Prog. Energy Combust. Sci. 39, 285–319.

Martins, M., Villalobos, U., Delclos, T., Armstrong, P., Bergan, P.G., Calvet, N., 2015. New concentrating solar power facility for testing high temperature concrete thermal energy storage. Energy Proc. 75, 2144–2149.

Peiró, G., Gasia, J., Miró, L., Prieto, C., Cabeza, L.F., 2016. Experimental analysis of charging and discharging processes, with parallel and counter flow arrangements, in a molten salts high temperature pilot plant scale setup. Appl. Energy 178, 394–403.

Punzón, A., Serranoa, A., Sánchez, F., Velasco, F., Preciado, I., González-Irusta, J.M., López-López, L., 2016. Response of a temperate demersal fish community to global warming. J. Marine Syst. 161, 1–10.

Rellosoa, S., García, E., 2015. Tower technology cost reduction approach after Gemasolar experience. Energy Proc. 69, 1660–1666.

Solar Millenium AG, 2008. The Parabolic Trough Power Plants Andasol 1 to 3. www.solarmillennium.de (accessed on July 07, 2017).

Trabelsi, S.D., Chargui, R., Qoaider, L., Liqreina, A., Guizani, A.A., 2016. Techno-economic performance of concentrating solar power plants under the climatic conditions of the southern region of Tunisia. Energy Convers. Manage. 119, 203–214.

Veerakumar, C., Sreekumar, A., 2016. Phase change material based cold thermal energy storage: Materials, techniques and applications – a review. Inter. J. Refrig. 67, 271–289.

Weinstein, L.A., Loomis, J., Bhatia, B., Bierman, D.M., Wang, E.N., Chen, G., 2015. Concentrating solar power. Chem. Rev. 115, 12797–12838.